

Least-Squares Reverse-Time Migration

Gang Yao* and Helmut Jakubowicz, Imperial College London

Summary

We present a matrix-based implementation of least-squares reverse-time migration in which the predicted data are generated using a modified source wavelet. We also show that the combination of the least-squares formulation and reverse-time migration leads to an estimate of the reflectivity which is consistent with a deconvolution imaging condition; this in turn provides higher-resolution and more accurate amplitudes than conventional reverse-time migration. The implementation described here is computationally efficient, but requires a large amount of memory and storage, and is not currently suitable for application in 3D.

Introduction

Migration attempts to produce an image of the subsurface by reversing the propagation effects in seismic data. Although in principle this requires the inverse of a modeling operator, in practice the adjoint of the modeling operator is used instead. In cases where the data are subject to significant aliasing, truncation, noise, or are incomplete, the adjoint modeling operator is not a good approximation to the inverse operator (Claerbout, 1992), and this degrades the resolution of the final migrated image.

An improved approximation to the inverse operator can be obtained using a least-squares approach (Nemeth et al., 1999; Kühl and Sacchi, 2001; Kaplan et al., 2010; Dai and Schuster, 2010). In this work we present a formulation of least-squares reverse-time migration (LSRTM) that is based on an explicit matrix representation of generalized diffraction-stack migration (Schuster, 2002). Our implementation of this method uses a modified source wavelet to perform the forward and inverse steps at each iteration, and is regularized using a roughness penalty constraint. This reduces the computation, but requires a relatively large amount of memory and storage. The results show increased resolution and improved amplitude treatment compared to conventional reverse-time migration (RTM).

Theory

Migration consists of three steps: forward modeling of the source wavefield, back propagation of the recorded data, and imaging. In RTM, forward modeling is achieved by solving the two-way wave equation, and, for a point source, can be expressed as

$$u_s(\mathbf{x}, \omega) = G(\mathbf{x}|\mathbf{x}_s; \omega) S(\omega), \quad (1)$$

where u_s is the modeled wavefield, G is the Green's function, S is the source signature, \mathbf{x} is position, \mathbf{x}_s is the source location, and ω is angular frequency. The recorded data, D , are then back-propagated into the subsurface using the adjoint of the modeling operator, G^\dagger , giving

$$u_r(\mathbf{x}, \omega) = \int G^\dagger(\mathbf{x}|\mathbf{x}_r; \omega) D(\mathbf{x}_r, \omega) d\mathbf{x}_r. \quad (2)$$

The imaging step generates an estimate of the reflectivity, $I(\mathbf{x})$, by relating u_s and u_r to each other at all points in the subsurface. This is normally done by correlating the wavefields and selecting the zero lag, and can be expressed in the frequency domain as

$$I(\mathbf{x}) = \int u_s(\mathbf{x}, \omega) u_r^\dagger(\mathbf{x}, \omega) d\omega, \quad (3)$$

where u_r^\dagger is the conjugate (time-reverse) of the back-propagated data. Substituting Equations 1 and 2 into Equation 3 then gives the basic equation of RTM:

$$I(\mathbf{x}) = \iint [G(\mathbf{x}|\mathbf{x}_s; \omega) S(\omega)] [G^\dagger(\mathbf{x}|\mathbf{x}_r; \omega) D(\mathbf{x}_r, \omega)]^\dagger d\omega d\mathbf{x}_r. \quad (4)$$

Since $I(\mathbf{x})$ is real, Equation 4 can be rewritten as

$$I(\mathbf{x}) = \iint [G(\mathbf{x}|\mathbf{x}_s; \omega) \sqrt{S(\omega)}]^\dagger [G(\mathbf{x}|\mathbf{x}_r; \omega) \sqrt{S(\omega)}] D(\mathbf{x}_r, \omega) d\omega d\mathbf{x}_r. \quad (5)$$

Equation 5 can be implemented as a three-stage matrix calculation as follows: first, the contributions from the Green's functions and source terms are obtained by solving the two-way wave equation using a source with a signature corresponding to $\sqrt{S(\omega)}$ (note that reciprocity then enables a single set of calculations to be used for both terms); second, the kernel in Equation 5 is evaluated by conjugating and multiplying (i.e. time-reversing and convolving) the terms in square brackets obtained from the first step, and then multiplying (convolving) the result with the recorded data; finally, all the traces and frequencies are summed together. This procedure corresponds to generalized diffraction-stack migration, and is equivalent to RTM (Schuster, 2002).

Equation 5 uses adjoints of forward-modeling operators, rather than inverse operators, and therefore only provides an estimate of the subsurface reflectivity. By comparison, the recorded data are directly related to the true reflectivity, $R(\mathbf{x})$, and can be described by

LSRTM

$$D(\mathbf{x}_r, \omega) = \iint [G(\mathbf{x}|\mathbf{x}_s; \omega)\sqrt{S(\omega)}][G(\mathbf{x}|\mathbf{x}_r; \omega)\sqrt{S(\omega)}] R(\mathbf{x}) d\mathbf{x}. \quad (6)$$

Equations 5 and 6 can be used to formulate an iterative least-squares scheme that produces an optimum estimate of the reflectivity which is consistent with the recorded data. This is done by minimizing the objective function

$$F(I) = \| < D > - D \|^2, \quad (7)$$

where $< D >$ represents the modeled data obtained from Equation 5 (corresponding to the estimated reflectivity), and D describes the recorded data.

The minimization of Equation 7 forms the basis of the LSRTM method used here, and is equivalent to finding the least-squares solution to Equation 6. Rewriting Equation 6 in matrix notation as

$$D = G_r G_s S R, \quad (8)$$

then the standard least-squares solution for R is given by

$$R = [(G_r G_s S)^\dagger (G_r G_s S)]^{-1} (G_r G_s S)^\dagger D. \quad (9)$$

which can in turn be shown to be equal to

$$R = [u_s]^{-1} u_r. \quad (10)$$

Equation 10 is equivalent to the deconvolution imaging condition of Valenciano and Biondi (2003) and describes the reflectivity as the ratio of the reflected and incident wavefields, rather than through their crosscorrelation. It follows that, in providing an optimum match between the data and reflectivity model, LSRTM also implements Valenciano and Biondi's deconvolution imaging condition. This has the additional benefit of making the resulting reflectivity independent of the source signature.

Implementation

The objective function given by Equation 7 can be minimized using a modified conjugate-gradient method (Scales, 1987). Because of the structure of Equation 5, this can be implemented using matrices constructed directly from the forward-modeling operator and its adjoint, together with a modified source signature corresponding to $\sqrt{S(\omega)}$. These matrices can be precomputed ahead of the migration, thereby providing an efficient implementation.

As in the case of conventional RTM, the use of a two-way wave equation can produce low-wavenumber artifacts which can be removed using a Laplacian filter after migration (Youn and Zhou, 2001). However, whereas the adjoint operator used in RTM is unconditionally stable, the

inverse required for LSRTM can still be ill-posed. This generates additional noise, but can be controlled using a roughness constraint (Bube and Langan, 2008).

Examples

We will demonstrate our implementation of LSRTM using two models. The first model consists of nine point diffractors embedded in a medium with a constant velocity of 2000 m/s (Figure 1a). Figure 1d shows a shot record from this model for a surface source at $x=450$ m, and receivers every 25 m along the surface; the source signature is a 30 Hz Ricker wavelet, and the direct arrivals, which do not contribute to imaging, have been removed. Figures 1b and 1c show the results of applying conventional RTM and LSRTM to the data in Figure 1d, while Figures 1e and 1f show the modeled data corresponding to the RTM and LSRTM images. In this case noise and instabilities are not an issue, and Laplacian filtering is not required; the LSRTM result also does not use a roughness constraint.

Figure 1 shows that LSRTM has two advantages relative to RTM. First, the diffractors in the LSRTM image have fewer sidelobes, and are better resolved than those from RTM. This is because the imaging condition for RTM is based on crosscorrelation, and therefore retains (actually amplifies) the imprint of the source signature. By contrast, in matching the image and recorded data, LSRTM effectively uses the deconvolution imaging condition given by Equation 10, and thereby compensates for the source signature. Second, the amplitudes of the later arrivals in the modeled LSRTM data are closer to those in the recorded data than in the case of RTM. This is because RTM uses adjoint, rather than inverse, operators, and these fail to correct adequately for geometrical spreading. In particular, in using an approximate inverse to describe the relationship between the image and recorded data, LSRTM provides a better representation of the amplitude effects related to propagation. This helps preserve the amplitudes inherent in the reflectivity, and leads to a more accurate image.

The second example uses the Marmousi model (Versteeg and Grau, 1991; Versteeg, 1993). Figure 2 shows the velocity and reflectivity models for the Marmousi data, while Figure 3a shows the shot record at source location $x=3000$ m, with receivers located between 425 m and 2800 m at intervals of 12.5 m. The RTM image from this shot record is shown in Figure 3b, and corresponds to the area enclosed within the red box in Figure 2a. In this case low-wavenumber artifacts arising from the use of the two-way wave equation are an issue, but can be removed using a Laplacian filter (Figure 3c). However, even after Laplacian filtering, the final RTM image retains high-wavenumber artifacts.

LSRTM

Figure 3d shows the image produced by LSRTM without a roughness constraint. Relative to conventional RTM, this implementation of LSRTM suppresses high-wavenumber artifacts and increases the resolution in the final image; however, it also contains a significant amount of high-wavenumber noise. Figure 3e shows the corresponding LSRTM result, but using a roughness constraint. This successfully removes the high-wavenumber noise, but retains low-wavenumber artifacts which are inherent in the numerical solution of the two-way wave equation. Finally, Figure 3f shows the result of applying a Laplacian filter to the data in Figure 3e. This image has fewer artifacts, is more highly resolved than that from RTM, and also has more consistent amplitudes over a wider area.

Figure 4 shows stacks of the images obtained by migrating fifteen shots across the Marmousi model using (a) conventional RTM after Laplacian filtering, and (b) LSRTM using a roughness constraint. Laplacian filtering was not used for the LSRTM result because stacking attenuated the low-wavenumber artifacts, and the residuals

were instead removed by a mild low-cut filter. Despite the limited number of shots, both stacks appear to be well resolved, although the amplitudes in the RTM result show a noticeable decrease with depth. By contrast, the amplitudes in the LSRTM result more closely match those of the true reflectivity model. This again demonstrates that LSRTM can provide more accurate images than RTM.

Conclusions

We have described a matrix formulation of reverse-time migration (LSRTM) that is based on generalized diffraction-stack migration, and can provide improved imaging relative to conventional RTM. Unfortunately, while this method is computationally efficient, it requires a large amount of storage, and is currently impractical for application in 3D. An alternative, non-linear formulation of least-squares reverse-time migration which retains the benefits of least-squares imaging, but is more suitable for 3D data, is described in a companion paper (Yao and Jakubowicz, 2012).

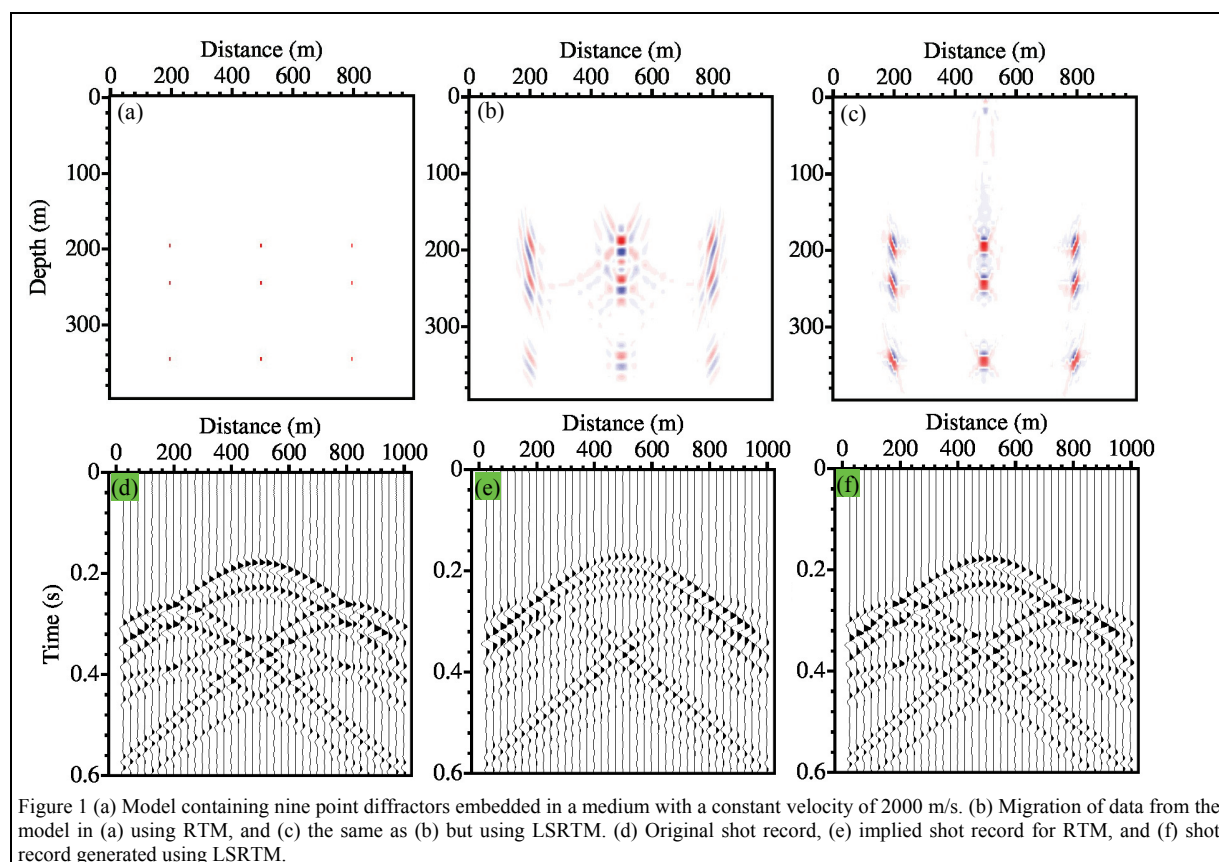
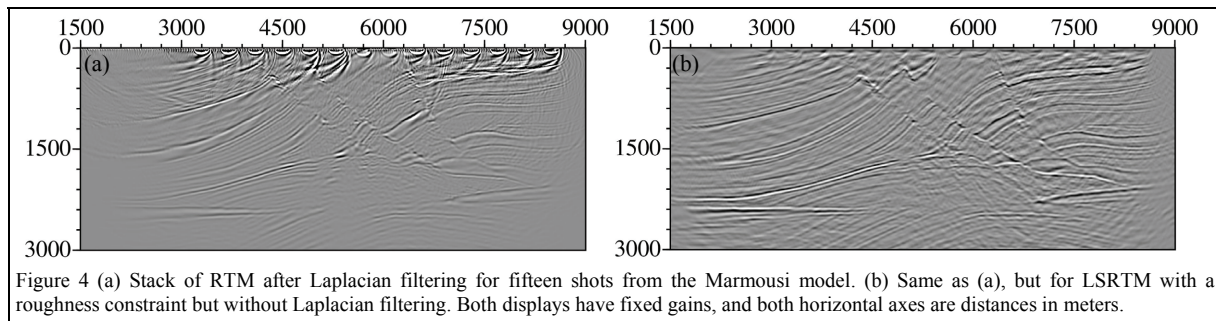
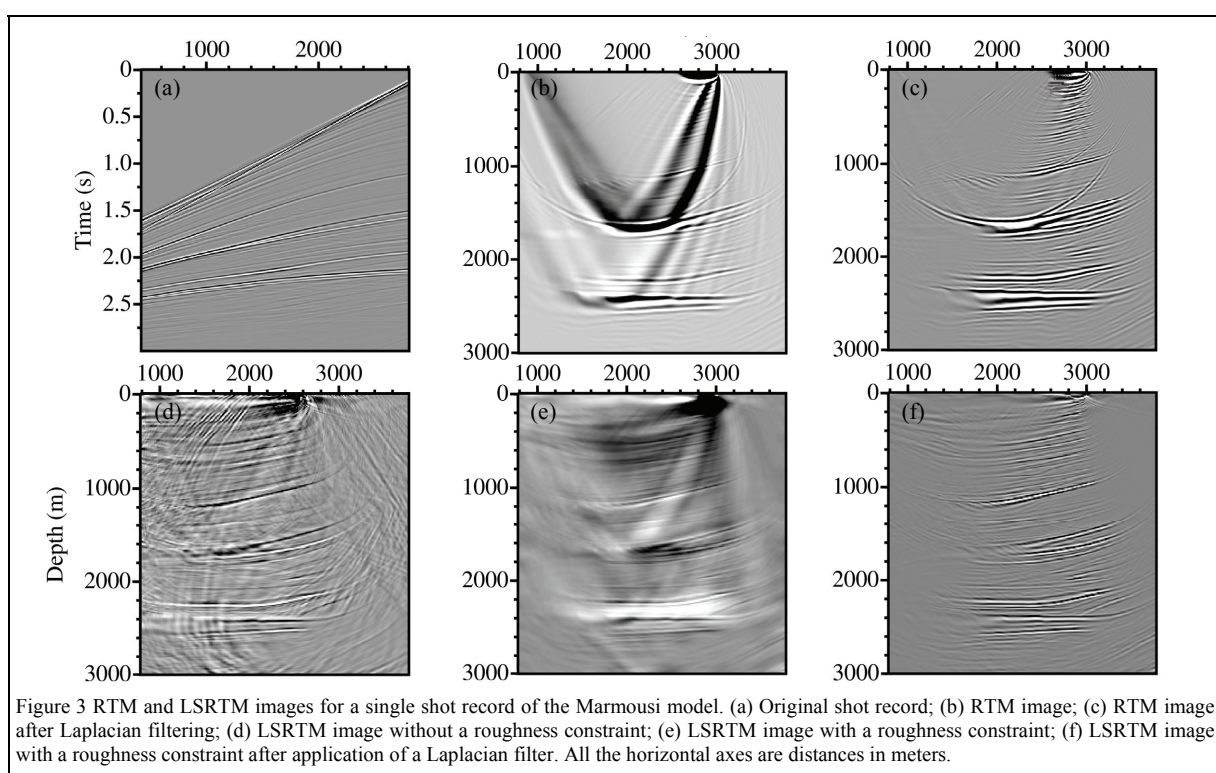
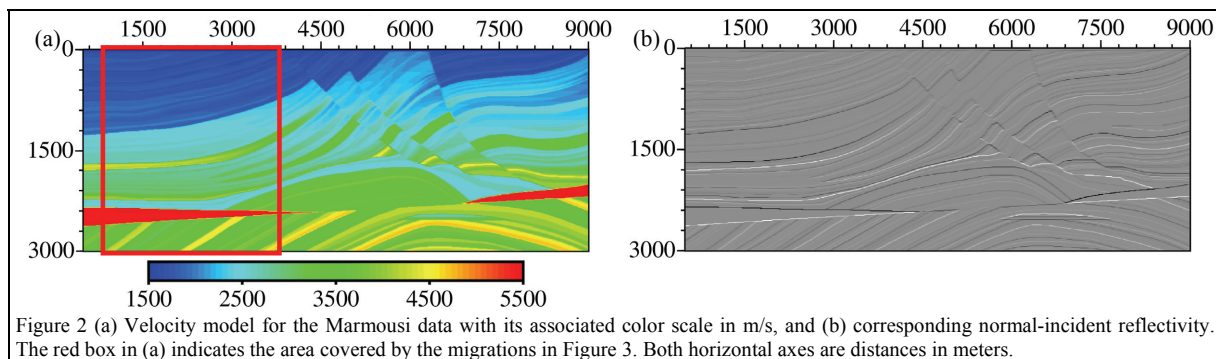


Figure 1 (a) Model containing nine point diffractors embedded in a medium with a constant velocity of 2000 m/s. (b) Migration of data from the model in (a) using RTM, and (c) the same as (b) but using LSRTM. (d) Original shot record, (e) implied shot record for RTM, and (f) shot record generated using LSRTM.

LSRTM



<http://dx.doi.org/10.1190/segam2012-1425.1>

EDITED REFERENCES

Note: This reference list is a copy-edited version of the reference list submitted by the author. Reference lists for the 2012 SEG Technical Program Expanded Abstracts have been copy edited so that references provided with the online metadata for each paper will achieve a high degree of linking to cited sources that appear on the Web.

REFERENCES

- Bube, K. P., and R. T. Langan, 2008, A continuation approach to regularization of ill-posed problems with application to Crosswell-traveltime tomography: *Geophysics*, **73**, no. 5, VE337-VE351.
- Claerbout, J. F., 1992, Earth soundings analysis: Processing versus inversion: Blackwell Science.
- Dai, W., and G.T. Schuster, 2010, Multi-source wave-equation least-squares migration with a Deblurring filter: 72nd Conference and Exhibition, EAGE, P276.
- Kaplan, S.T., P. S. Routh, and M. D. Sacchi, 2010, Derivation of forward and adjoint operators for least-squares shot-profile split-step migration: *Geophysics*, **75**, no. 6, S225-S35.
- Kühl, H., and M. D. Sacchi, 2001, Generalized least-squares DSR migration using a common angle imaging condition: 71st Annual International Meeting, SEG, Expanded Abstracts, 1025-28.
- Nemeth, T., C. Wu, and G. T. Schuster, 1999, Least-squares migration of incomplete reflection data: *Geophysics*, **64**, 208-221.
- Scales, J.A., 1987, Tomographic inversion via the conjugate gradient method: *Geophysics*, **52**, 179-85.
- Schuster, G.T., 2002, Reverse-time migration = generalized diffraction stack migration: 72nd Annual International Meeting, SEG, Expanded Abstracts, 1280-1283.
- Valenciano, A. A., and B. Biondi, 2003, 2-D deconvolution imaging condition for shot-profile migration: 73rd Annual International Meeting, SEG, Expanded Abstracts, 1059-1062.
- Versteeg, R.J., 1993, Sensitivity of prestack depth migration to the velocity model: *Geophysics*, **58**, 873-882.
- Versteeg, R.J., and G. Grau, eds., 1991, The Marmousi experience: EAGE, workshop on practical aspects of seismic data inversion (Copenhagen, 1990).
- Yao, G., and H. Jakubowicz, 2012, Non-linear least-squares reverse-time migration: Abstract submitted for presentation at the 82nd Annual International Meeting, SEG.
- Youn, O. K., and H. Zhou, 2001, Depth imaging with multiples: *Geophysics*, **66**, 246-255.